Hydrogen Bonding Versus Electrostatic Driving Forces of Phosphate Binding at the Air - Water Interface

Research Thesis

Presented in partial fulfillment of the requirements for graduation *with research distinction* in Chemistry in the undergraduate College of Arts and Sciences of The Ohio State University

By

Alexander Grooms

The Ohio State University

April 2019

Project Advisor:

Dr. Heather C. Allen

Department of Chemistry and Biochemistry

ABSTRACT

There is an increasing need to understand the principles of phosphate recognition. Phosphate is in high demand due to fertilizer and biofuel production but supplies are limited because of depleting phosphorus rock mines. Eutrophication caused by agricultural runoff leaves the human phosphate cycle open and devastates aquatic ecosystems. Aqueous phosphate recognition and recycling could play an important role in energy conservation, food security, and water management. Phosphate recognition also has biological applications in adenosine triphosphate binding. However the principles of aqueous phosphate capture are not well understood. Langmuir monolayers at the air – water interface provide a unique environment to study the physical properties and chemical driving forces of phosphate binding. An amphiphilic receptor with an ammonium headgroup (**U-Ammo**$^+$) and a receptor with a guanidinium headgroup (**U-Guan**$^+$) were employed in this study. **U-Ammo**$^+$ provides pure electrostatic binding interactions through the charged dimethyl ammonium headgroup, and **U-Guan**$^+$ provides both hydrogen bonding and electrostatic interactions through the charged guanidinium headgroup. The binding constants were determined for both molecules using surface sensitive infrared analysis at 5.5 °C and 31.5 °C via a Langmuir-type fit. The binding constants were used with temperature in Van't Hoff equations to obtain enthalpy, entropy, and free energy of phosphate binding. Overall **U-Guan**$^+$ had larger binding constants and free energy driving forces than **U-Ammo**$^+$, suggesting **U-Guan**$^+$ is a better phosphate receptor. Both receptor-phosphate binding showed enthalpy as the main driving force. **U-Guan**$^+$ showed less entropic hindrance to binding suggesting preorganization. **U-Guan**$^+$ has previously shown selectivity up to 1:1000 phosphate-chloride while in this study, **U-Ammo**$^+$ showed minimal phosphate selectivity at 1:1 phosphate-chloride concentration.

ACKNOWLEDGEMENTS:

I would like to thank Jennifer Neal for the support and assistance in designing and performing the experiments for this study, the editing and counseling provided in the writing of this thesis, as well as continued mentorship through three years of undergraduate research. I would also like to thank the Allen group for their mentorship and feedback on my project and Dr. Heather Allen for presenting me with the opportunity to perform academic research in the field of my choice. Lastly, I would like to thank the Department of Chemistry and Biochemistry and the Undergraduate Research Office at The Ohio State University for financial and educational support.

PUBLICATIONS:

Neal, J. F.; Zhao, W.; Grooms, A. J.; Flood, A. H.; Allen, H. C. Arginine-Phosphate Recognition Enhanced in Phospholipid Monolayers at Aqueous Interfaces. *J. Phys. Chem. C* **2018**.

Neal, J. F.; Zhao, W.; Grooms, A. J.; Smeltzer, M. A.; Shook, B. M.; Flood, A. H.; Allen, H. C. Interfacial Supramolecular Structures of Amphiphilic Receptors Drive Aqueous Phosphate Recognition. *In Review.* **2019.**

Table of Contents

CHAPTER 1: MOTIVATIONS AND BACKGROUND

1.1 Phosphate Demand

Phosphorus is an integral component of a growing and delicate system of water management, energy conservation, and food security in modern global society.[1] Biofuel production depends on the usage of phosphorus, and biofuels are increasingly important for alternative energy sources.[1] However, phosphorus rock is a limited and non-renewable natural resource.[1,2] Reserves of phosphorus rock are predicted to be depleted in the next 50 to 100 years, with United States supplies limited to 30 years.[2] In addition to these constraints, remaining phosphorus rock reserves are largely located in politically and economically unstable parts of the world (such as Morocco's Bou Craa mine in the Western Sahara), and therefore will take increasing energy and money to mine and transport.[2]

With growing populations, there is an increasing need for higher food production. This will require more efficient agricultural industries with higher crop yield per unit area of cultivation.[2] Phosphorus, and its aqueous form phosphate, is an important constituent of modern agricultural fertilizers along with nitrogen, sulfurous, and potassium.[2] In the context of this research, the term phosphate will be used to refer to $H_2PO_4^-$, which is the major species present in unpolluted, natural waters.[3] Because phosphorus rock is limited, there is a critical need for anthropogenic phosphate recycling.[2,4] Recycling agricultural phosphate has the potential to decrease the energy used in fertilizer production and increase the availability of phosphate for fertilizer production, which has increasing demand with growing populations.[4]

1.2 The Human Phosphorus Cycle and Eutrophication

It is necessary to sequester and recycle phosphate used in agricultural fertilizers to effectively close the human phosphorus cycle. When phosphate-based fertilizers or manure applications (which are high in phosphate[5]) are used on crops, there is an excess of phosphate deposited in the surface levels of the soil.[2,5] Surface phosphate transfers to water sources via rain or irrigation in a process known as agricultural runoff.[5,6] Phosphate pollution comes from a number of agricultural sources and not a single definable source, therefore it is referred to as a non-point source of pollution.[7,8] The natural phosphorus cycle cannot efficiently process the high amounts placed by agriculture. When excess phosphate departs the cycle through agricultural runoff and erosion, the cycle is left open.[6,8]

The consequence of runoff from non-point agricultural sources is increased amounts of aqueous phosphate in water sources such as ponds, lakes, rivers, deltas, and shorelines. [7,9,10] The amount and conditions of phosphate runoff vary depending on season and location, but the concentration ranges from 0.1 to 0.5 mg/L which corresponds to ~10 μM.[5,11,12] The pH conditions associated with runoff conditions are between pH 4.5 to 8.[11,12] The majority of this range corresponds to the $H_2PO_4^-$ speciation of aqueous phosphate, which was employed within this study. [3,13]

Excess amounts of phosphate induce a phenomenon known as eutrophication in which large amounts of aquatic algae grow and coat the water's surface.[8–10] Phosphate is the limiting factor in eutrophication, as this nutrient promotes the growth of biologically simple algae over more complex aquatic plant life.[9,10] When algal blooms progress and begin to die, the decomposition of the bloom depletes aqueous oxygen via cellular respiration.[7,9,10,14] The lowered oxygen levels in the waters causes the death of other aquatic life, leading to areas known as

"dead zones" where the ecosystem has been decimated.[7,9,10] As a result, there is a heightened need to reduce anthropogenic phosphate pollution. This ecosystem remediation would result in cleaner water supplies for drinking, and less economic and energetic strain in cleaning/aiding areas affected by algal blooms and dead zones.[9,10,15]

1.3 The Principles and Challenges of Phosphate Recognition

The need for anthropogenic phosphate remediation is complimented by the continued need to better understand the physical-organic principles behind phosphate recognition.[15] Phosphate binding can occur through two fundamental intermolecular interactions. Electrostatic interactions may occur between the negative charge on phosphate and a positive charge on a receptor. Also, hydrogen bonding may occur between the O-H groups on the phosphate and a complementary hydrogen bond acceptor/donor. Both of these interactions have been shown as important factors for strong, selective binding phosphate over other anions in solution.[16–18]

Selective phosphate binding in an aqueous environment comes with the challenge of a large energetic penalty for phosphate dehydration, which has a ΔG_{hyd} of -465 kJ/mol.[19] Another complication interfering with binding between a phosphate guest and receptor host is the large dielectric constant (ε) of bulk water ($\varepsilon = 80$).[3,20,21] The dielectric constant is an important factor in intermolecular binding interactions because it is the quantity by which Coulombic force between charges are shielded. A higher dielectric constant corresponds to more Coulombic shielding between positive and negative charges and therefore less effective interactions.[21,22] Phosphate also has a large size to charge ratio that is resultant of the singular negative charge delocalized over the large phosphate molecule.[3,20] One last complication in phosphate binding is the acid/base qualities of triprotic phosphate, resulting in multiple possible species of phosphate

in solution depending on the pH.[3,13] The pK_a's of phosphate are $pK_{a1} = 2.16$, $pK_{a2} = 7.21$, and $pK_{a3} = 12.32$.[23]

There is a literature precedence of using guanidinium receptors in low dielectric constant environments provided by organic solvents, such as DMSO for the recognition of phosphate.[16,24–28] A specific technique that has recently been investigated is the guest-host interactions of phosphate-guanidinium at the air-water interface, which benefits from a decreased dielectric environment[18,21]. This technique will be subsequently discussed in more detail. A principle of phosphate recognition that has not been extensively studied is the thermodynamic driving forces behind the binding process.

1.4 Objectives

A primary goal for this project is to compare the driving forces for phosphate binding to amphiphilic receptors at the air – water interface. The guest-host intermolecular interactions that occur between negatively charged phosphate, a positively charged receptor, and a positively charged receptor with hydrogen bond donors will be understood. This will be evaluated at the air - water interface due to the decreased dielectric constant present at the interface.[21,22] It will be determined qualitatively whether hydrogen bond-assisted electrostatic interactions between guest and host are more effective than pure electrostatic binding. Furthermore, an investigation of whether a hydrogen bond-assisted electrostatic binding receptor will provide phosphate selectivity over a pure electrostatic binding receptor. Lastly, the binding coefficients between host-guest association will be quantified along with enthalpy of binding ($\Delta H°$), entropy of binding ($\Delta S°$), and free energy of binding ($\Delta G°$). The specific theory and technique that will be employed to meet these objectives will be discussed in Chapter 2.

CHAPTER 2: THE AIR – WATER INTERFACE AND PHOSPHATE BINDING

2.1 Benefits of Interfacial Water

The large ε of bulk water suggests that significant charge shielding occurs.[3,20] The lessening of positive and negative electrostatic interaction along with positive and negative dipole interaction found in hydrogen bonding is what makes water an excellent solvent, however it also greatly inhibits host-guest binding.[21,22,29] The high ε of bulk water has been attributed to the large degree of rotational freedom that the molecules possess in unconfined space.[21] The ability for water dipoles to rotate freely suggests that bulk water has high electric polarizability – or has the potential to reorient dipoles in the presence of an electric field. Charges and partial charges on molecules in aqueous solution act as small electric fields - thus free-rotating bulk water molecules may align around the field forming a solvation shell, solvating the charged molecule, and preventing it from firmly binding to another charged species in solution.[29,30]

A recent experimental study has given support to theoretical studies that the ε of water greatly decreases at interfaces.[21] When water molecules are confined near an interface they lose a large degree of rotational freedom and align dipoles at the surface, which results in a decrease of the ability to align in an electric field.[31–33] Decreased polarizablity suggests that interfacial water does not act to shield charges as much as bulk water. Consequently, the magnitude of the dielectric constant depended greatly on the thickness of the confined water layers ranging from ε = 2 in the thinnest layers to ε ~ 20 at thicker interfacial water.[21] An additional study indicates that electrostatics govern the affinity between anions and cations in solvents with low dielectric constants.[30] These previous findings are important in the context of this study because the low

dielectric constant of surface water at the air – water interface will be taken advantage of, along with the amphiphilic design of positively charged receptors, to sequester and bind negatively charged phosphate at the surface.

2.2 Langmuir Monolayers and Surface Pressure – Area Isotherms

A Langmuir monolayer describes the two dimensional environment when a thin film is spread over the surface of water. These films are often comprised of amphiphilic molecules with long, hydrophobic, alkyl chains and a hydrophilic headgroup. These molecules orient at the air – water interface with the hydrophobic tails pointing away from the water and the hydrophilic headgroup interacting with the surface layers of water. Langmuir monolayers provide multiple benefits that lead to improved binding at the air – water interface. First, monolayers have been utilized because of their self-organization and confined micro-environment.[34,35] The pre-organized environment of self-aligning molecules at the surface of water allow for optimization of the molecular design – improving the molecule's performance in binding.[35,36] A benefit realized from the preorganization of Langmuir monolayers is an enthalpically favorable binding region.[36,37] The preorganization of the monolayer means that less energy is needed to place the guest and the host into the proper orientation for binding. Multiple studies have taken advantage of these benefits to investigate the binding of guests to the monolayer hosts.[38–41]

Surface Pressure – Area (Π-A) Isotherms are an analytical technique utilized in the study of Langmuir monolayers. Π-A isotherms measure the Π of a monolayer film as a function of mean-molecular area. The underlying physical principle behind the isotherm is that as the mean molecular area between amphiphilic molecules oriented at the surface of water decreases, the surface pressure will increase, which packs the long hydrophobic tails in closer proximity. The

molecules are spread onto the surface of water in what is known as the gaseous phase. This occurs at high mean molecular areas, where there is a low degree of hydrophobic tail organization, loose molecular packing, and low surface pressure. When the molecules are compressed to a specific mean molecular area, they enter the condensed phase in which the molecules begin to attain order, and the tails are not as free as in the gas phase. Lastly, at low mean molecular area, the molecules enter the collapse phase in which the tails are well ordered and packed closely together. In previous studies, Π-A isotherms have been used to observe binding events by monitoring the expansion in mean molecular area at a given surface pressure, which arises due to differing monolayer ordering/organization between bound and unbound states.[18,42–44] One of the amphiphiles used in this study was adopted from Neal *et. al.* The design of this receptor will be discussed later, but it is important to note that this molecule showed no mean molecular area expansion which was attributed to the long alkyl chains masking any monolayer re-ordering due to binding.

2.3 Infrared Reflection Absorption Spectroscopy

Infrared Reflection Absorption Spectroscopy (IRRAS) is a useful method to investigate structural information and understand binding affinities at the air – water interface. This technique brings the advantages of infrared spectroscopy to the surface of water, allowing the identification of functional groups in molecules at the surface. Infrared light perturbs molecular vibrations that result in an oscillating dipole moment, which is characteristic of specific types of vibrations in a bond between atoms.[45]

A typical IRRAS setup will have an infrared beam reflected from a mirror and onto the surface of a Langmuir monolayer, then back to a mirror and into the detector. Data from IRRAS

is reported as reflectance-absorbance (RA) versus wavenumber, where RA is defined by the following equation.

$$RA = -log_{10}(\frac{R}{R_o}) \quad (1)$$

Where R is the reflectivity of the surface of water with the Langmuir monolayer on top of it, and R_o is the reflectivity of pure water.

Phosphate containing compounds have been extensively studied via IRRAS and have yielded well-defined characteristic frequencies of phosphate vibrations.[35,45–48] Two modes of high interest in this study are the phosphate PO_2^- asymmetric stretch that occurs ~ 1220-1250 cm^{-1} and the phosphate PO_2^- symmetric stretch that occurs ~ 1090 cm^{-1}.[45,48] Additionally, it has been observed that the PO_2^- symmetric stretch can be shifted to higher frequency (blue-shifted) depending on the degree of dehydration of phosphate.[49] In previous studies by Neal *et. al*, the presence of PO_2^- symmetric and asymmetric stretching frequencies have been observed to change based on the concentration of aqueous phosphate, suggesting binding between phosphate moieties and guanidinium moieties at the air – water interface[18] (in review).

2.4 Receptor Structure and Function in Phosphate Recognition

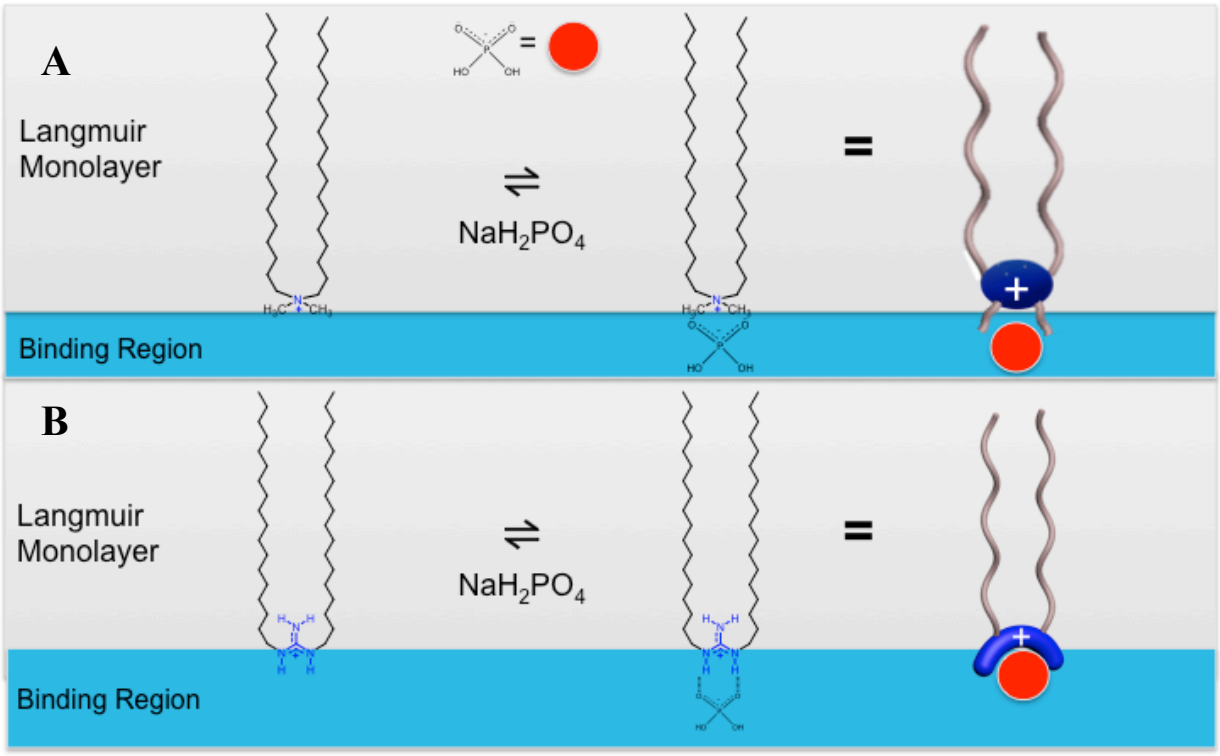

Figure 1: Proposed binding motif at the air – water interface for U-Ammo$^+$-phosphate binding (A) and U-Guan$^+$-phosphate binding (B)

The amphiphilic receptors in this study were chosen based on the unique intermolecular driving forces for binding that each receptor offers at the air – water interface. The receptor in **figure 1A**, dimethyldioctadecylammonium bromide (**U-Ammo**$^+$), was chosen due to the pure electrostatics at the ammonium head group and the double octadecyl alkyl chain for monolayer formation. The interactions of the **U-Ammo**$^+$ molecule with phosphate are purely electrostatic due to the lack of hydrogen bond donor sites at the ammonium head group – therefore, the only interaction that may occur is between the negatively charged phosphate molecule and the positively charged ammonium.

The receptor in **figure 1B** , cationic dioctadecylguanidinium (**U-Guan**$^+$), was designed by Neal *et al* (in review) and chosen for the molecule's unique ability of the guanidinium head group to interact with phosphate via electrostatics and hydrogen bonding. There is a large

literature precedent for the binding of guanidinium to phosphate, which include the biological inspiration of ATP and AMP binding to guanidinium functional groups.[24,28,38,50–53] This interaction has been considered successful due to the electrostatic attraction between negatively charged phosphate and positively charged guanidinium, and the hydrogen bond donors on guanidinium interacting with the hydrogen bond acceptors on phosphate. The ability for phosphate and guanidinium to interact via hydrogen bonding in addition to electrostatics suggests that phosphate should selectively bind to the **U-Guan**$^+$ receptor over the **U-Ammo**$^+$ receptor. The thermodynamic driving forces behind the binding of phosphate to a receptor at the air – water interface are not well understood. Furthermore, the effect of hydrogen bond-assisted electrostatic binding versus pure electrostatic binding at the air – water interface has not been investigated.

2.5 A Thermodynamic Approach to Phosphate – Receptor Binding

As stated, the thermodynamic driving forces of interfacial phosphate binding are largely unexplored, however the energetics of binding to a guanidinium host in bulk water, organic solvent sub-phase, and at the solid – liquid interface can be applied to determine useful thermodynamic quantities.[54–57] Changes in free energy of binding (ΔG_b), enthalpy of binding (ΔH_b), and entropy of binding (ΔS_b) can give detailed information about driving forces behind phosphate binding and quantitative support to the proposed binding models for the **U-Ammo**$^+$ and **U-Guan**$^+$ receptors. It may be determined whether hydrogen bond-assisted electrostatic binding results in a more spontaneous binding event than pure electrostatic driven binding, and which thermodynamic component (enthalpy or entropy) is the principle driving force.

A bulk study of phosphate binding to guanidinium and ammonium host in water depended largely on the solvent shell of the complex.[54] Binding to the ammonium host was driven by entropy change due to the release of the solvation shell upon binding – overcoming unfavorable (endothermic) enthalpy change, and binding to the guanidinium host was driven by (exothermic) enthalpy change due to the pre-organized structure of the guanidinium host.[54] This pre-organization in conjunction with a less hydrated environment caused the guanidinium guest and phosphate host to be in a favorable binding pocket, and therefore binding occurred with enthalpy as the driving force.[54] This result can be compared to the pre-organized and confined setting of a Langmuir monolayer at the air – water interface providing a favorable environment for enthalpy driven binding.[36,37] Another study found that receptors capable of forming bi-dentate hydrogen bonds with hosts demonstrated exothermic binding and favorable entropy change.[55] This study was performed in DMSO with a lower dielectric constant (ε ~ 40), which is comparable to the significantly decreased dielectric constant at the surface of water, thus amplifying phosphate binding via increased electrostatic interactions.[21,22]

In order to determine the thermodynamic quantities of phosphate binding to U-Ammo+ and U-Guan+ receptors, the binding constant must first be determined at a series of temperatures. The association binding coefficient, K_a will be obtained using the general Langmuir model in **equation 2** and the assumption that the phosphate to receptor binding occurs at a 1:1 ratio. This assumption has been previously made due to the nature of the binding 'pocket' created by the hydrogen bond donors of the **U-Guan**$^+$ receptor (**figure 1B)**.

$$I = I_{max} \frac{[phosphate]}{(1/K_a)+[phosphate]} \quad (2)$$

In this equation, I is the integration of the asymmetric PO_2^- stretching frequency after water intensity subtraction and I_{max} is the maximum integration of the stretching frequency. K_a is the

association binding constant. A larger K_a correlates to a stronger guest-host bind. K_a may be related to ΔG_b at a specific temperature via the following thermodynamic principle where R is the gas constant (8.314 J/K mol).[57–59]

$$\Delta G_{b,T} = -RTlnK_a \quad (3)$$

Equation 3 may be rearranged to form **equation 4** using **equation 5** to obtain the Van't Hoff equation of a line. Through Van't Hoff plots the natural log of the binding coefficient can be displayed as a function of inverse temperature in **equation 4** where ΔH_b is in J/mol and ΔS_b is in J/mol K.[57–59]

$$\ln K_a = -\frac{\Delta H_b}{RT} + \frac{\Delta S_b}{R} \quad (4)$$

$$\Delta G_b = \Delta H_b - T\Delta S_b \quad (5)$$

The values for ΔH_b can be obtained from the slope of the Van't Hoff line ($-\Delta H_b/RT$) and ΔS_b can be obtained from the y-intercept of the Van't Hoff line ($\Delta S_b/R$) in the plot of ln K_d versus 1/T. The value of Gibbs free energy change at a given temperature $\Delta G_{b,T}$ may be obtained by inserting ΔH_b and ΔS_b into **equation 5**, the principle equation of thermodynamics.[57]

CHAPTER 3: MATERIALS AND METHODS

3.1 Materials

The materials used in this study were purchased with the exception the **U-Guan**$^+$ receptor. This receptor was designed and synthesized in conjunction with Indiana University (Wei Zhao). Multiple stock solutions of **U-Guan**$^+$ stock solution were made in a 4:1 mixture of chloroform:methanol (HPLC grade, Fisher Scientific). Multiple stock solutions of

dimethydioctadecylammonium bromide (U-Ammo+) (>99%, Acros Organics) were made in chloroform (HPLC grade, Fisher Scientific). Sodium dihydrogen phosphate monobasic monohydrate (≥99.5%, Sigma) and sodium chloride (ACS grade Fisher, baked at 650 °C for > 8 hours prior to use) was dissolved in ultra pure water that had a resistivity of 18.2 MΩ cm (A10 Advantage) to form varying concentrations of stock phosphate solutions. The pH of the highest concentration phosphate solution was 5.185.

3.2 Methods

3.2.1 Surface Pressure – Area Isotherms

Although Π-A isotherms were not used in the determination of phosphate binding coefficients, the technique was necessary in IRRAS and useful for the concentration calibration of the **U-Ammo**$^+$ and **U-Guan**$^+$ receptor solutions. Π-A isotherms were completed on a customized Teflon Langmuir trough, which had an area of 144.5 cm^2 and movable Delrin compression barriers (KSV NIMA, Finland). The cleaning procedure for the trough and the barriers was rigorous in order to avoid contamination from which surface sensitive techniques are prone. To ensure cleanliness for each trial, a quick compression of the subphase in the trough was performed before each trial and the Π did not rise above 0.2 mN/m suggesting that there was no surfactant contamination.

For the collection of Π-A isotherms, surface pressure was monitored using the Wilhelmy plate method with custom cut filter paper plates (Ashless grade, Whatman). These plates were soaked in ultrapure water for one minute before being placed on the surface tensiometer. KSV software (KSV, Finland) controlled the surface pressure, and receptor monolayers were spread drop-wise onto the aqueous surface in the trough using a microsyringe (Hamilton). The syringe

was cleaned thoroughly with reagent alcohol, allowed to air dry, and then cleaned ten times with chloroform (HPLC grade, Fisher). Ten minutes elapsed before the start of each trial to allow for solvent evaporation of the receptor spread solution. The barriers were compressed at a constant speed of 5 mm/min for each barrier. When the surface pressure was reached (40 mN/m) the barriers were oscillated at 1 mm/min in order to maintain constant Π.

Figure 2: Experimental setup with Langmuir trough, barriers, Wilhelmy plate, and temperature probe in the FTIR with an IRRAS mirror setup

3.2.2 Infrared Reflection Absorption Spectroscopy

IRRAS was the principle technique used in this study to obtain phosphate-binding data. A Fourier transform infrared (FTIR) spectrometer (Spectrum 100, PerkinElmer) was used to collect all spectra. This FTIR had a liquid nitrogen cooled HgCdTe (MCT) detector that was filled prior to each experiment. The Langmuir Π-A setup was placed on a breadboard that also had two gold-plated mirrors – each of which were precisely set in order to collect reflectivity of IR light off of the monolayer surface at a 46 ° angle of incidence.

The Langmuir Π-A setup was also connected to a Julabo MC temperature control system (Julabo Labortechnik, Germany). Rubber tubing pumped heated or cooled water through the interior of the trough, placing the sub-phase and monolayer at a desired temperature. For this study, experimental temperatures were maintained at 5.5°C and 31.5 °C. The temperature controller was set at 1 °C and 37 °C to obtain these temperatures, which were measured with a temperature probe through the software that was placed into the sub-phase and secured to the FTIR. To avoid contamination, the probe was cleaned thoroughly with reagent alcohol after every trial and allowed to dry completely.

IRRAS background spectra were collected off of the sub-phase substance with no monolayer and off of the surface of the monolayer at 40 mN/m for each trial. All spectra were performed immediately after the surface pressure reached 40 mN/m for consistency and to prevent any relaxation that may occur over time. IRRAS spectra were recorded by averaging 300 scans, which were collected using unpolarized light and the single-beam mode of the FTIR. The spectra were plotted as reflectance-absorbance (RA), which was given by **equation 1**, versus frequency. Data analysis was performed using Origin software (OriginLab 9, Northampton, MA). Each spectrum shown represents the average of three identical experiments.

CHAPTER 4: RESULTS AND DISCUSSION

4.1 U-Ammo^{+}–Phosphate Interactions at the Air – Water Interface

4.1.1 ***U-Ammo***$^{+}$ *Receptor IRRAS*

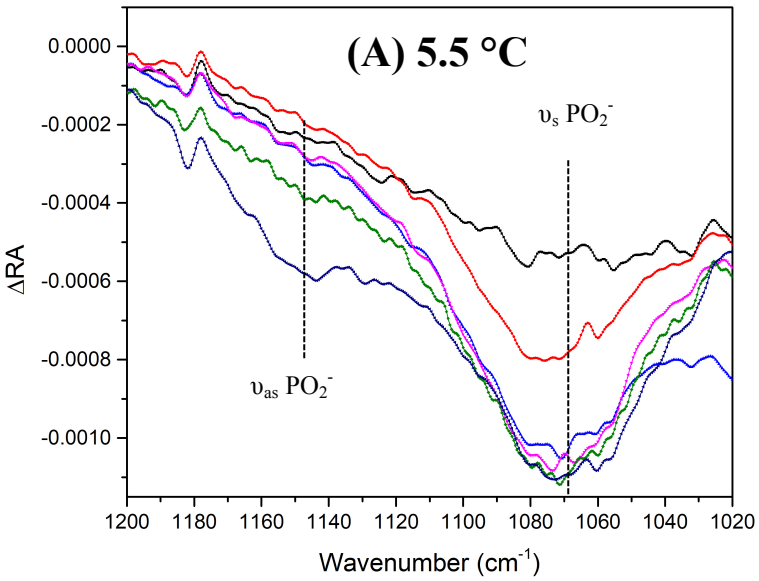

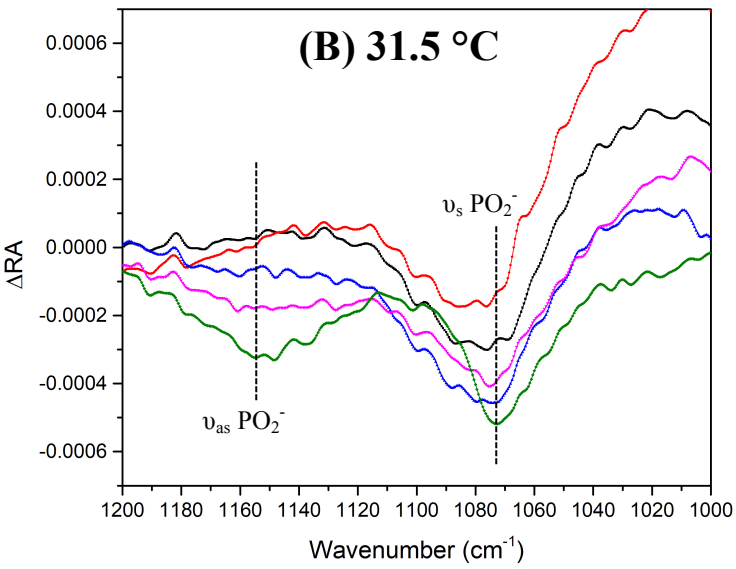

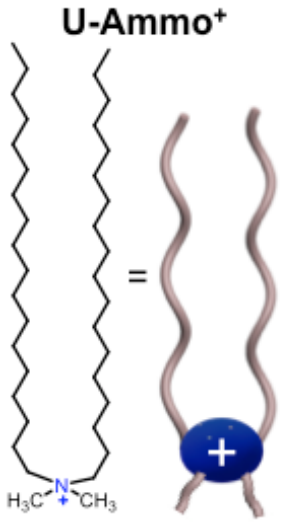

Figure 3: IRRAS spectra of U-Ammo^{+} on phosphate at 5.5 °C (A) and 31.5 °C (B)

A principle goal of this project was to observe and quantify binding between the receptor's head group guest and aqueous $H_2PO_4^-$ host at different temperatures. The coupling of IRRAS and temperature control allowed for spectroscopic exploration of these binding interactions at 5.5 °C and 31.5 °C (**Figure 3**). These IRRAS spectra were collected at a Π of 40 mN/m, which corresponded, to the well-organized condensed phase of the receptor monolayer. The phosphate PO_2^- stretching frequency has been shown as a binding-sensitive region.[60] This is supported here where the PO_2^- symmetric stretch and the PO_2^- asymmetric stretch, which have been assigned at 1071 cm^{-1} and 1150 cm^{-1} respectively[61,62], increase in relative intensity with increasing phosphate concentration. If no phosphate-receptor binding was present then the phosphate modes would not appear via IRRAS due to the nature of the reflectance-absorbance equation. In this equation, the IRRAS spectrum of the receptor monolayer on phosphate sub-phase is divided by spectrum of the phosphate sub-phase - thus acting to normalize any free aqueous phosphate modes. The presence of these modes suggests that phosphate is being attracted to the receptor monolayer at the surface of water. The spectra in **Figure 3** have also had the spectra of the receptor on pure water subtracted in order to emphasize the phosphate binding peaks.

The 10,000 μM phosphate spectra in **Figure 3A** (dark blue) at 5.5 °C shows the PO_2^- symmetric mode with a peak height of ~0.0008 ΔRA and a peak width of ~100 cm^{-1}. The 10,000 μM phosphate spectra in **Figure 3B** (green) at 31.5 °C shows the same mode with a peak height of ~0.0004 ΔRA and peak width of ~110 cm^{-1}. This decrease in intensity and broadening of the

peak is a temperature effect that is in accordance with a Boltzmann distribution. At a higher temperature, more vibrational microstates are being probed due to a higher energy system.

4.1.2 ***U-Ammo***$^{+}$ *Receptor Binding Affinity*

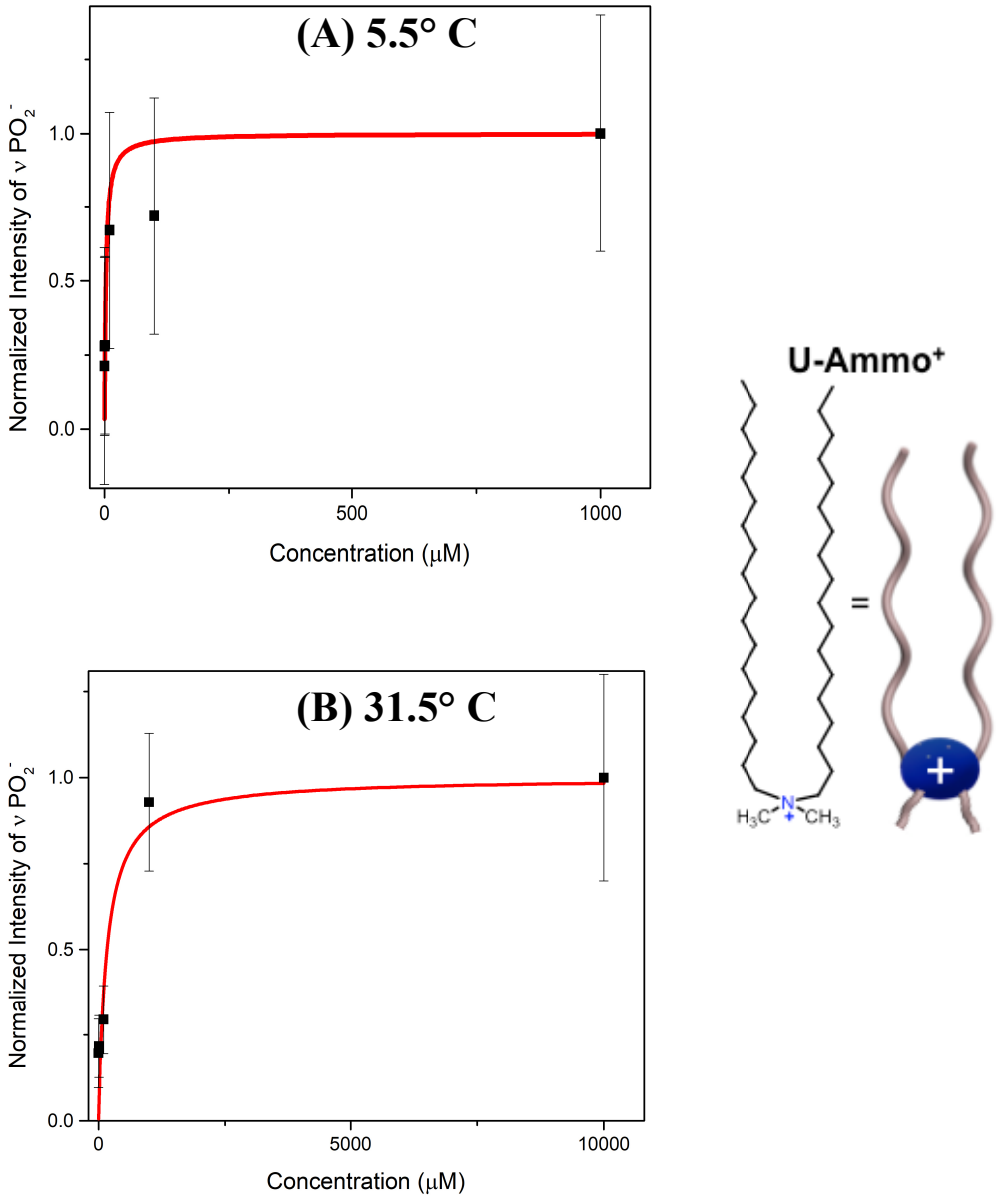

Figure 4: U-Ammo^{+}-phosphate normalized PO_2^- stretch at 5.5 °C (A) and 31.5 °C (B) showing an increase in intensity with phosphate addition until binding site saturation.

U-Ammo^{+}-phosphate binding at 5.5 °C and 31.5 °C was quantified by plotting the normalized intensity of the full PO_2^- stretch versus concentration of phosphate (**Figure 4**). The lower temperature was integrated from 1019 cm^{-1} to 1200 cm^{-1} and the high temperature was integrated from of 992 cm^{-1} to 1200 cm^{-1} in order to account for the peak broadening observed at the higher temperature. The peak integration of pure water was subtracted from each of the phosphate concentrations and was then normalized by dividing by the maximum peak intensity. Due to this normalization, "0" represents the intensity of **U-Ammo**$^{+}$ on water and "1" represents the highest PO_2^- intensity in the probed region. This data was then fit to the general Langmuir model (equation 2) to quantify K_a and plotted to obtain the binding curves. The error bars in **figure 4** represent the propagated error of the standard deviation of three identical trial integrations, subtraction of water intensity, and normalization division. **Figure 4A** shows the Langmuir fit of **U-Ammo**$^{+}$ binding to phosphate at 5.5 °C, which yielded a binding affinity of $K_a = 3.62\times10^5 \pm 2\times10^5$ M^{-1}. The Langmuir fit of **U-Ammo**$^{+}$-phosphate binding at 31.5 °C seen in **figure 4B** gave a binding affinity of $K_a = 5.9\times10^3 \pm 3\times10^3$ M^{-1}. This decrease in magnitude suggests that the **U-Ammo**$^{+}$ receptor becomes significantly worse at binding to phosphate at higher temperatures. Additionally, a larger K_a at low temperatures suggests that enthalpy is the principle driving force of binding – with binding being less favorable at higher temperature, more energetic environments.

*4.1.3 Thermodynamic Driving Forces of **U-Ammo**$^{+}$-phosphate Binding*

T	K (M^{-1})	1/T	ln K	error
278.5 K	3.62×10^{5}	0.00359	12.799	±0.54
304.5 K	5.9×10^{3}	0.00328	8.683	±0.50

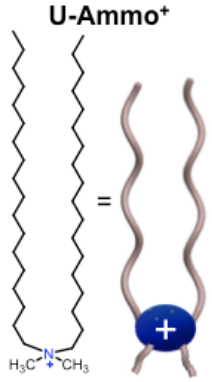

Figure 5: U-Ammo^{+} Van't Hoff data from which the $\Delta H°_b$ and the $\Delta S°_b$ were respectively obtained.

The thermodynamic driving forces of **U-Ammo**$^{+}$ binding to phosphate may be quantified via Van't Hoff analysis (**figure 5**), in which the two points may approximate the slope of the line. The K_a obtained from the Langmuir fit, assuming 1:1 phosphate-receptor binding, may be visualized as a binding equilibrium constant between bound and unbound states (equation 7,8).

$$U - Ammo^{+} + H_2PO_4^{-} \rightleftharpoons U - Ammo{:}\,H_2PO_4 \quad (7)$$

$$K_a = \frac{(UAmmo{:}H_2PO_4)}{(UAmmo^{+})(H_2PO_4^{2-})} \quad (8)$$

Where K_a may be used to obtain ΔH_b, ΔS_b, and $\Delta G_{b,T}$ through the Van't Hoff equation (equations 2-6).[57–59] A summary of thermodynamic quantities may be seen in **Table 1**.

U-Ammo$^+$					
$K_{a,5.5° C}$ (M^{-1})	$K_{a,31.5° C}$ (M^{-1})	ΔH_b (J/mol)	ΔS_b (J/mol K)	$\Delta G_{5.5° C}$ (J/mol)	$\Delta G_{31.5° C}$ (J/mol)
3.62×10^5	5.9×10^3	-1621	-4.27	-429.2	-318.2

Table 1: Thermodynamic values for U-Ammo$^+$-phosphate binding

The negative ΔH_b and negative ΔS_b of **U-Ammo**$^+$ binding to phosphate suggests that this binding process is enthalpically driven rather than entropically driven. The negative ΔS_b may be explained in the context of this binding environment because the un-bound system yields more microstates, where as the bound system is more ordered with fewer microstates. Upon binding the system become more organized overall and therefore causes an unfavorable negative entropy change. The expected enthalpic driving force is a product of the benefits of Langmuir monolayers at the air-water interface creating a low ε environment in which electrostatic interactions dominate anion binding.[30,36,37] The negative ΔG_b at both high and low temperature display that receptor-phosphate binding is spontaneous, but more so at the lower temperature, which is another product of enthalpy driven binding. It should be noted that a third data point will be obtained at 15 °C in order to confirm the Van't Hoff analysis used herein.

4.2 U-Guan$^+$–Phosphate Interactions at the Air – Water Interface

4.2.1 ***U-Guan***$^+$ *Receptor IRRAS*

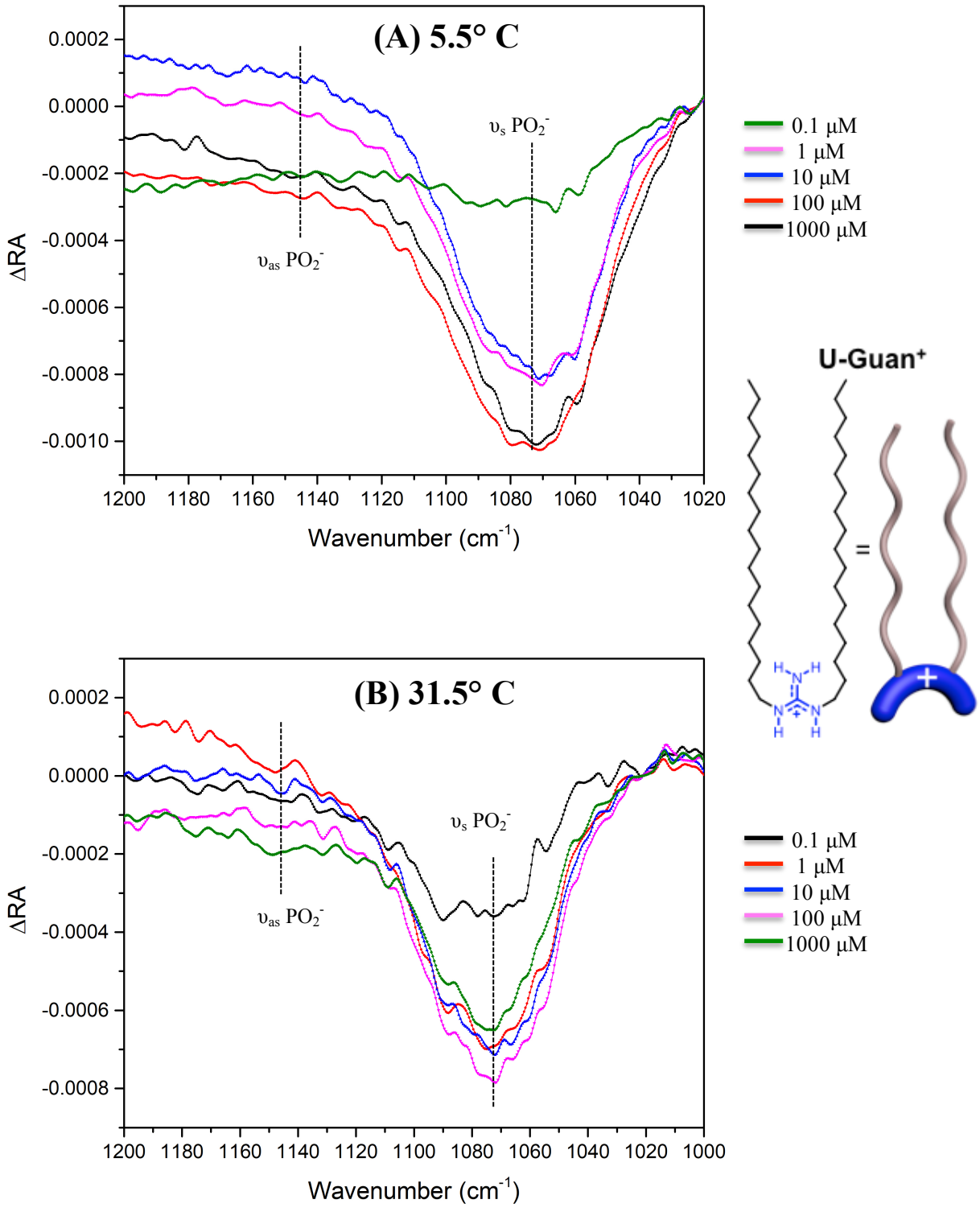

Figure 6: IRRAS spectra of U-Guan$^+$ on phosphate at 5.5 °C (A) and 31.5 °C (B)

IRRAS spectra of the **U-Guan**$^+$ receptor at 5.5 °C and 31.5 °C on a range of phosphate concentration sub-phases were utilized to determine **U-Guan**$^+$-phosphate binding in the same manner as discussed for the **U-Ammo**$^+$ receptor (**figure 6**). These spectra have again had the water spectrum subtracted from each phosphate spectrum and are therefore plotted as ΔRA versus wavenumber. The PO_2^- symmetric stretch again occurs at 1071 cm^{-1} and varies with phosphate concentration. It is seen that at high concentrations the binding of phosphate to **U-Guan**$^+$ becomes saturated, as the PO_2^- symmetric stretch of the 1 μM phosphate solution has similar relative intensity to the 10,000 μM solution for both low and high temperatures. These similar intensities suggest that the number of binding sites quenched at a low sub-phase phosphate concentration, which could be attributed to the hydrogen bond-assisted electrostatic interactions between the guanidinium head group and $H_2PO_4^-$. The temperature effect on the infrared peaks is again observed as a broadening of the PO_2^- symmetric stretch from 5.5 °C (**figure 6A**) to 31.5 °C (**figure 6B**).

*4.2.2 **U-Guan**$^+$ Receptor Binding Affinity*

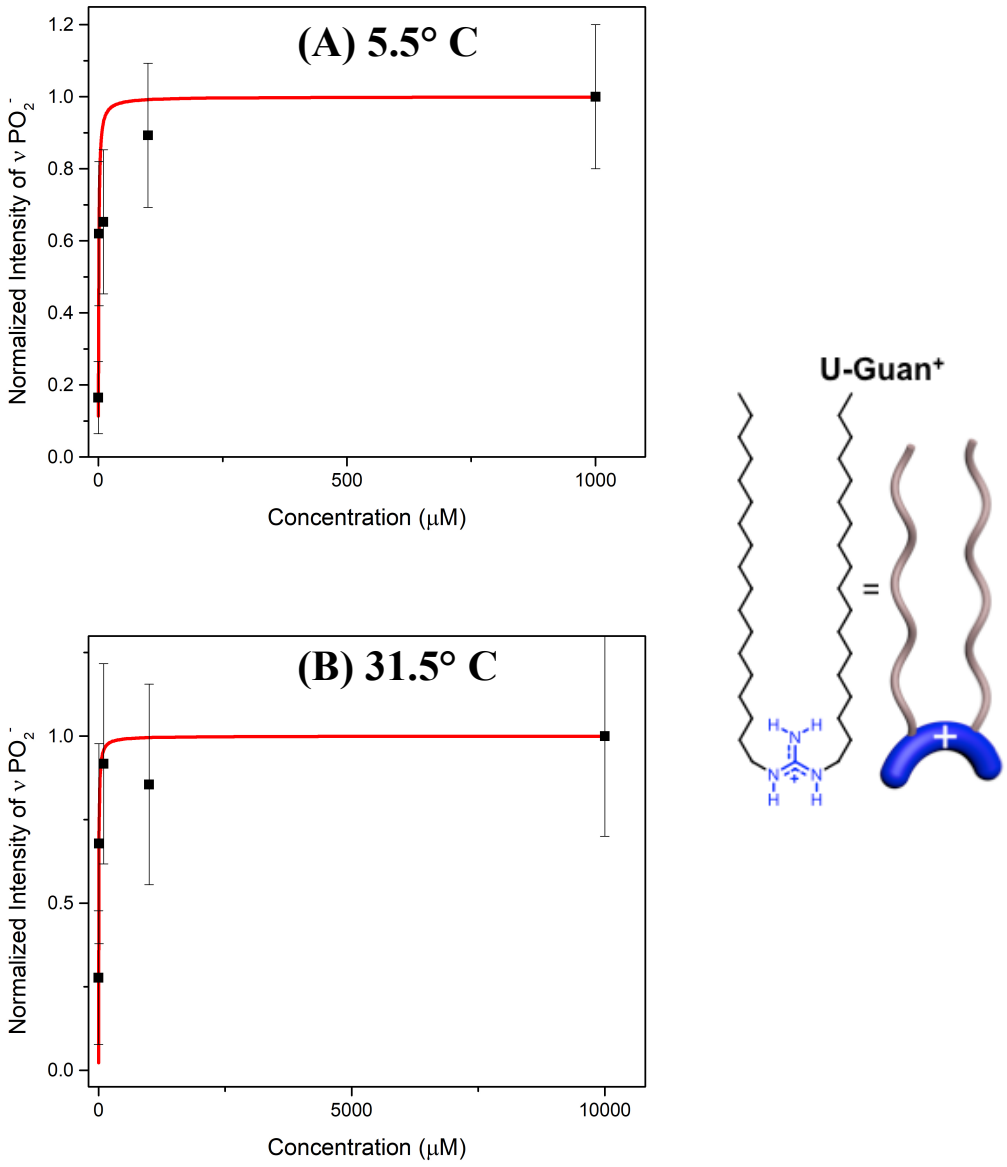

Figure 7: U-Guan^{+}-phosphate normalized PO_2^- stretch at 5.5 °C (A) and 31.5 °C (B) showing an increase in intensity with phosphate addition until binding site saturation.

The K_a for phosphate binding to **U-Guan^{+}** was again quantified using the general Langmuir fit by integrating the phosphate PO_2^- stretch (**figure 7**). To account for the temperature effect, the more narrow peak of the 5.5 °C spectra were integrated from 1019-1200 cm^{-1} (**figure**

7A), and the more broad 31.5 °C peak from 992-1200 cm^{-1} (**figure 7B**). The integration of each PO_2^- peak again had the spectral intensity of water subtracted and were normalized to the maximum intensity. The error associated with the averaging of three spectra per phosphate concentration was propagated through the subtraction of water intensity and the division of the maximum intensity normalization. The value of K_a for **U-Guan**$^+$-phosphate binding at 5.5 °C and 31.5 °C was determined to be $1.3\times10^6 \pm 0.7\times10^6$ M^{-1} and $2.3\times10^5 \pm 1\times10^5$ M^{-1} respectively. The magnitude of K_a is again higher at the lower temperature suggesting an enthalpically driven binding process. At the higher temperature the receptor does not bind phosphate as well due to the excess thermal energy present in the system.

*4.2.3 Thermodynamic Driving Forces of **U-Guan**$^+$-phosphate Binding*

T	K (M^{-1})	1/T	ln K	error
278.5 K	1.29×10^6	0.00359	14.069	±0.55
304.5 K	2.26×10^5	0.00328	12.329	±0.68

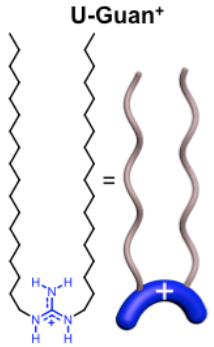

Figure 8: U-Guan$^+$ Van't Hoff data from which the $\Delta H°_b$ and the $\Delta S°_b$ were respectively obtained.

Assuming 1:1 binding for the **U-Guan**$^+$ receptor to phosphate, the K_a for binding may be modeled as a chemical equilibrium between bound and unbound states (equations 9,10).

$$UGuan^+ + H_2PO_4^- \rightleftharpoons UGuan{:}H_2PO_4 \quad (9)$$

$$K_a = \frac{(UGuan{:}H_2PO_4)}{(UGuan^+)(H_2PO_4^{2-})} \quad (8)$$

As seen with the **U-Ammo**$^+$ receptor the K_a for **U-Guan**$^+$ binding at both low and high temperatures are of large magnitude therefore suggesting that the equilibrium lies heavily to the right, favoring the bound state over the unbound state. The slope of a line may be approximated from the two points in **figure 8**, and used with the Van't Hoff equations (equations 2-6) to obtain ΔS_b from the y-intercept and ΔH_b from the slope of the line. As before, a third data point at 15 °C will be obtained to confirm the equation of the line used herein. The ΔG_b may then be obtained at each temperature, the summary of which may be seen in **Table 2.**

U-Guan$^+$					
$K_{a,5.5° C}$ (M^{-1})	**$K_{a,31.5° C}$ (M^{-1})**	**ΔH_b (J/mol)**	**ΔS_b (J/mol K)**	**$\Delta G_{5.5° C}$ (J/mol)**	**$\Delta G_{31.5° C}$ (J/mol)**
1.3×10^6	2.3×10^5	-685	-0.763	-472.0	-452.3

Table 2: Thermodynamic values for U-Guan$^+$-phosphate binding

This binding system is also enthalpically driven and entropically hindered as observed in the **U-Ammo**$^+$ binding system. The unfavorable negative ΔS_b may be attributed to the rearrangement that must occur upon the phosphate binding to the receptor in the monolayer – transitioning from a less ordered and unbound system to a more ordered and bound system. However once again the favorable negative ΔH_b drives the binding and is created by the low ε of the air – water interface,

thus allowing for electrostatic and hydrogen bond attractions between the guanidinium and phosphate to proceed unhindered.

4.3 Comparison of U-Ammo$^+$ and U-Guan$^+$ Affinity for Phosphate

	$K_{a,5.5^\circ C}$ (M^{-1})	$K_{a,31.5^\circ C}$ (M^{-1})	ΔH_b (J/mol)	ΔS_b (J/molK)	$\Delta G_{5.5^\circ C}$ (J/mol)	$\Delta G_{31.5^\circ C}$ (J/mol)
U-Ammo$^+$	3.62×10^5	5.9×10^3	-1621	-4.27	-429.2	-318.2
U-Guan$^+$	1.3×10^6	2.3×10^5	-685	-0.763	-472.0	-452.3

Table 3: Summary of Thermodynamic Data for U-Ammo$^+$ and U-Guan$^+$ Receptors

The thermodynamic quantities for phosphate binding may be compared (**table 3**) in order to propose which receptor is energetically more favorable to sequester phosphate at the air – water interface. A comparison of receptor K_a magnitudes can give the first insight that **U-Guan$^+$** is the better phosphate receptor. The magnitudes of K_a for **U-Guan$^+$** are at least one order of magnitude larger than **U-Ammo$^+$** at both high and low temperature. In comparing the enthalpic driving forces, both receptors have negative ΔH_b indicating enthalpy is the main driving force, however it may be seen that **U-Ammo$^+$** has the larger enthalpic driving force. One way that this may be explained, through electrostatic attraction, is that the positive charge on the guanidinium head group is delocalized between three nitrogen constituents of the functional group via resonance. This charge delocalization may act to slightly decrease the electrostatic potential of the group, creating a smaller electrostatic potential difference between $H_2PO_4^-$ and **U-Guan$^+$**. In contrast the positive charge on the ammonium head group is not delocalized via resonance

suggesting a larger electrostatic potential difference between $H_2PO_4^-$ and **U-Ammo$^+$** - giving rise to more enthalpically favored binding.

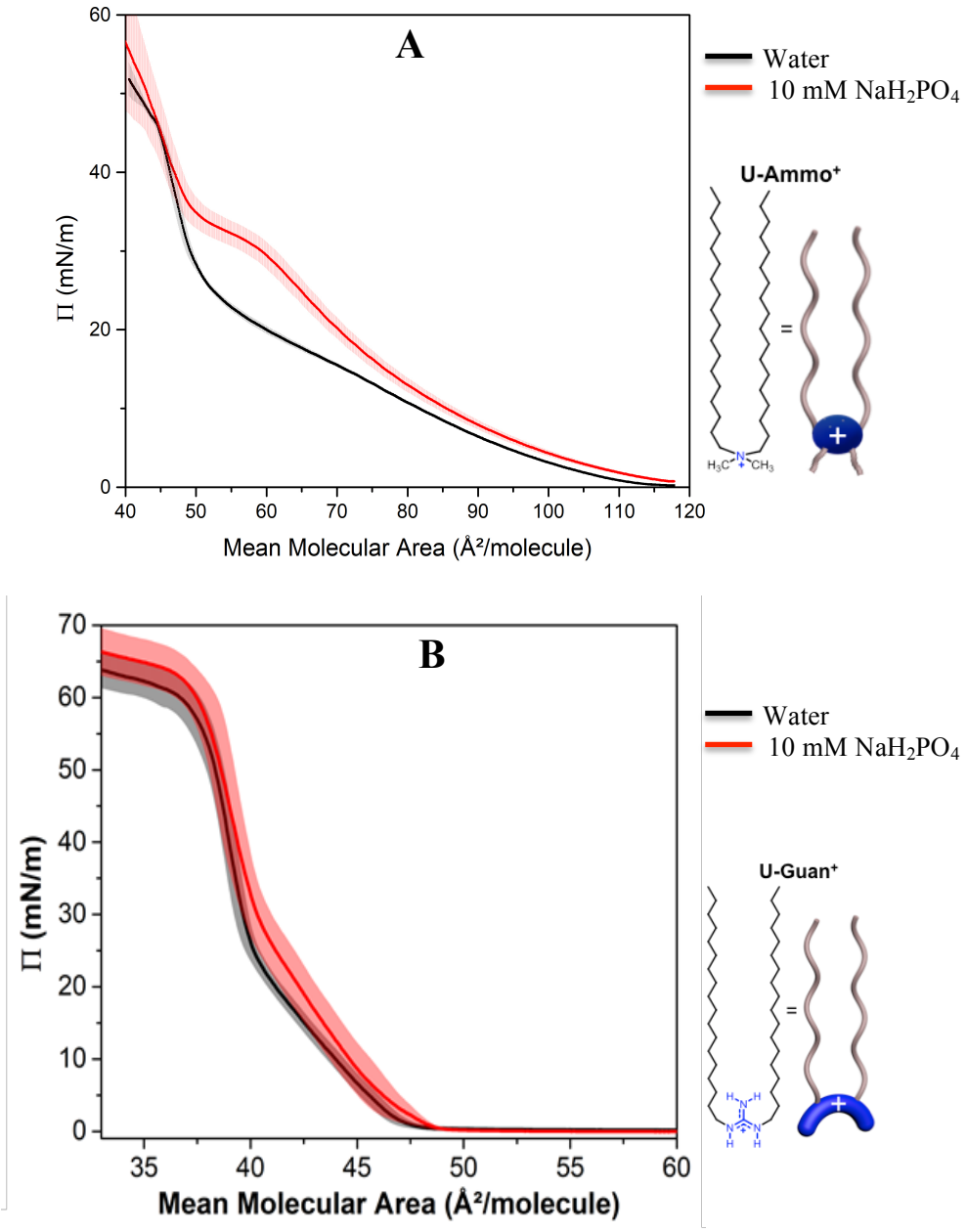

Figure 9: Π-A isotherms on water and 10 mM phosphate at 21 °C for U-Ammo$^+$ (A) and U-Guan$^+$ (B, from Neal 2019 *et. al* in review) with shaded regions representing one standard deviation above and below the average of three trials.

In analysis of ΔS_b it may be seen that binding in this unique environment is entropically unfavorable for both receptors. However ΔS_b for **U-Guan**$^+$ is less negative than for **U-Ammo**$^+$ suggesting that entropic hindrance is less of a barrier for the former binding than the latter. This may be explained via a discussion of the organization of the Langmuir monolayer and visualized using the Π-A isotherms of both receptors on water and phosphate subphases (**figure 9**). The isotherms of **U-Ammo**$^+$ on 10 mM phosphate show a large expansion in mean molecular area from the isotherm on water (**figure 9A**). This is contrasted by the isotherms of **U-Guan**$^+$ on water and phosphate (from Neal *et. al* 2019, in review), which show minimal expansion (**figure 9B**). An increase in mean molecular area upon phosphate binding to **U-Ammo**$^+$ suggests that the monolayer had to reorganize and reorient in order to bind phosphate. This reorganization may be a product of the bulky methyl groups at the ammonium head group, thus resulting in a larger entropic barrier to phosphate binding. The **U-Guan**$^+$ shows minimal expansion upon phosphate binding, suggesting that the monolayer did not have to reorganize. The preorganization of the guanidinium group with the hydrogen bond donors has been taken advantage of before for phosphate capture[16,24,25,50] - a property that is observed here as well. A lack of the need for monolayer reorganization and reorientation and the presence of hydrogen bond donors for phosphate binding to **U-Guan**$^+$ suggest that this receptor has a lower entropic barrier, which is experimentally supported by the less negative magnitude of ΔS_b. In comparing the values for $\Delta G_{b,T}$ it may be seen that enthalpic driving force of **U-Guan**$^+$ electrostatic binding coupled with the lower entropic barrier of binding due to organization and hydrogen bond donors in the guanidinium group result in **U-Guan**$^+$ having more negative $\Delta G_{b,T}$ overall than **U-Ammo**$^+$. A more negative $\Delta G_{b,T}$ suggests that **U-Guan**$^+$ is a better phosphate receptor than **U-Ammo**$^+$.

4.4 Anion Selectivity of Receptors Between Chloride and Phosphate Anions

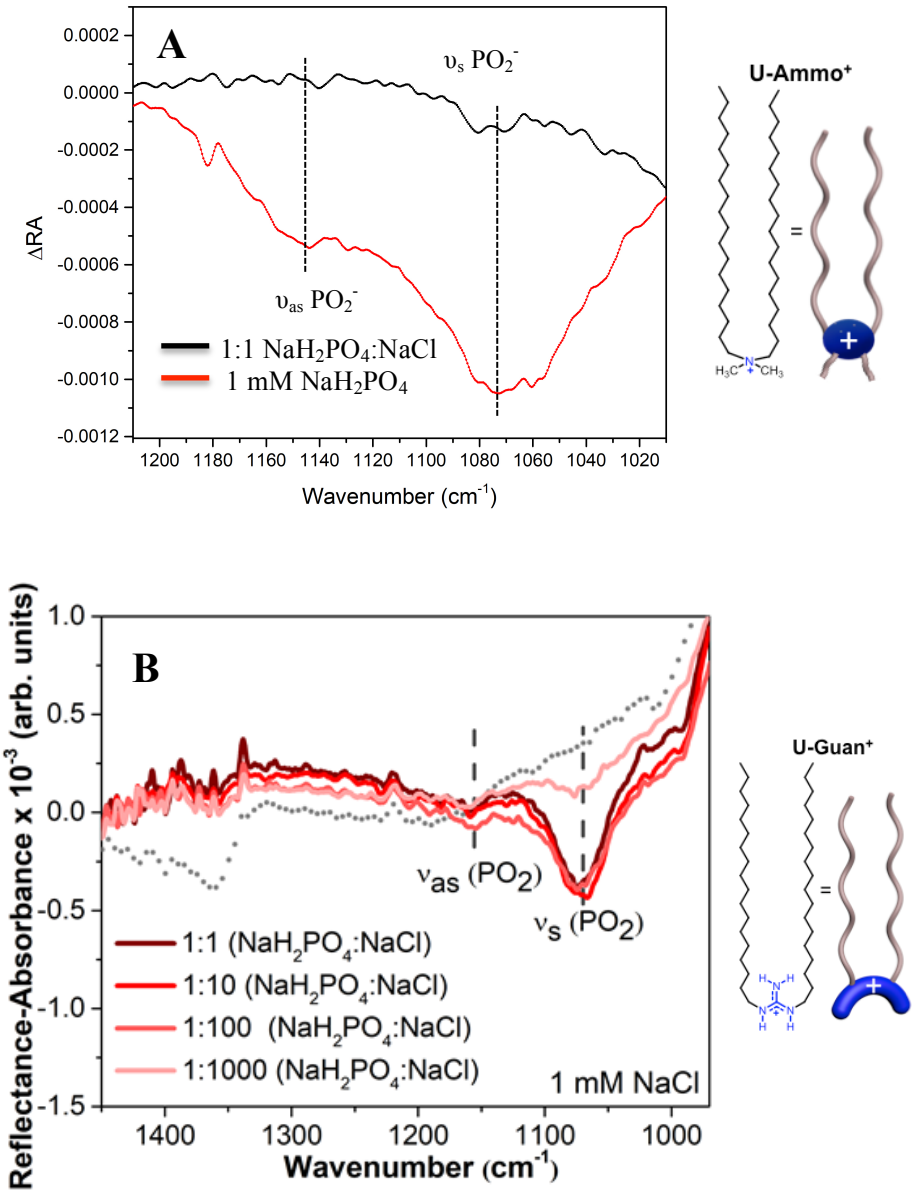

Figure 10: U-Ammo$^+$ on 1 mM phosphate to 1 mM chloride IRRAS compared to 1 mM phosphate IRRAS showing a decrease in PO_2^- stretching intensity with chloride addition (A) and U-Guan$^+$ IRRAS on varying ratios of phosphate to chloride showing selectivity up to 1:1000 (B, from Neal 2019 *et. al* in review).

The hydrogen bond-assisted electrostatics of the phosphate binding to **U-Guan**$^+$ not only make the receptor more energetically favorable, but also makes the receptor selective to phosphate over other anions such as chloride in solution (**Figure 10**). **Figure 10A** shows that the PO_2^- IRRAS stretch for **U-Ammo**$^+$ has significantly decreased in intensity in a 1 mM chloride to 1 mM phosphate solution compared to a 1 mM phosphate solution in which the PO_2^- symmetric and asymmetric bands are clearly visible. The decrease in intensity in the 1:1 phosphate-chloride solution suggests that **U-Ammo**$^+$ is binding to chloride anions rather than phosphate anions. This is likely the result of the pure electrostatics available for binding at the ammonium head group preferring chloride, a smaller anion with a more localized negative charge, over $H_2PO_4^-$, a larger anion with a delocalized negative charge. The opposite is observed for **U-Guan**$^+$ in a phosphate selectivity study by Neal *et. al,* 2019 (in review) in which **U-Guan**$^+$ shows selectivity for $H_2PO_4^-$ over chloride even at 1:1000 ratios of phosphate to chloride sub-phase concentration (**Figure 10B**). The selectivity of **U-Guan**$^+$ binding to phosphate is a product of the hydrogen bond-assisted electrostatic interactions of this receptor preferentially binding to the hydrogen bond acceptor sites on $H_2PO_4^-$. The high phosphate selectivity suggests that **U-Guan**$^+$ is a better phosphate receptor than **U-Ammo**$^+$ in an aqueous environment with both chloride and phosphate anions.

CHAPTER 5: CONCLUSIONS AND FUTURE WORK

There is a growing need to understand the principles and driving forces of aqueous phosphate capture. Phosphorus is integral to water management, energy conservation, and food security. With limited supplies of phosphorus rock and a growing demand for fertilizers to feed

an increasing world population there is a need to capture and recycle anthropogenic phosphate that is lost to water sources through agricultural runoff. Additionally, the eutrophication ignited by phosphate in water sources is a growing environmental danger and in need of remediation. In order to close the human phosphorus cycle, the principles and challenges of phosphate recognition must be understood and overcome. Studying phosphate capture at the air – water interface via Langmuir monolayers provides benefits for binding studies. Two amphiphilic molecules **U-Ammo**$^+$ and **U-Guan**$^+$ were studied at the interface via IRRAS to determine the driving forces of phosphate capture and to compare a pure electrostatic binding receptor, **U-Ammo**$^+$, to a hydrogen bond-assisted electrostatic binding receptor, **U-Guan**$^+$. Association binding constants for these two molecules were determined at 5.5 °C and 31.5 °C via a general Langmuir fit. Van't Hoff analysis then allowed the enthalpy of binding and entropy of binding to be determined for both molecules, which allowed quantification of the free energy of binding at low and high temperature. The **U-Guan**$^+$ receptor proved a thermodynamically better phosphate receptor than **U-Ammo**$^+$ due to the overall larger binding constants and more negative free energy driving force. Additionally, the phosphate selectivity of both receptors were qualitatively determined based upon IRRAS. It was shown that the **U-Ammo**$^+$ receptor was not selective to phosphate at 1:1 phosphate to chloride aqueous concentrations, and a previous study showed that **U-Guan**$^+$ is selective to phosphate over chloride up to 1:1000 $H_2PO_4^-$ to Cl^- ratios. This suggests that the **U-Guan**$^+$ receptor is also a better phosphate recognition receptor due to its ability to selectively bind phosphate via hydrogen bond-assisted electrostatic interactions. Future work for this project that is required includes collecting more thermodynamic data to gain more confidence in the results presented herein. The implications of these results are a contribution to

the understanding the principles of phosphate recognition for the further development of better phosphate receptors.

CHAPTER 6: REFERENCES

(1) Jarvie, H. P.; Sharpley, A. N.; Flaten, D.; Kleinman, P. J.; Jenkins, A.; Simmons, T. The Pivotal Role of Phosphorus in a Resilient Water–Energy–Food Security Nexus. *J. Environ. Qual.* **2015**, *44 (4)*.

(2) Cordell, D.; Drangert, J. O.; White, S. The Story of Phosphorus: Global Food Security and Food for Thought. *Glob. Environ. Chang.* **2009**. *19 (2)* 292-305.

(3) Deliomeroglu, M. K.; Lynch, V. M.; Sessler, J. L. Conformationally Switchable Non-Cyclic Tetrapyrrole Receptors: Synthesis of Tetrakis(1H-Pyrrole-2-Carbaldehyde) Derivatives and Their Anion Binding Properties. *Chem. Commun.* **2014**, *50(80)*, 11863–11866.

(4) Springmann, M.; Clark, M.; Mason-D'Croz, D.; Wiebe, K.; Bodirsky, B. L.; Lassaletta, L.; de Vries, W.; Vermeulen, S. J.; Herrero, M.; Carlson, K. M.; et al. Options for Keeping the Food System within Environmental Limits. *Nature* **2018**. *562(7728)*, 519–525.

(5) Elrashidi, M. A.; Mays, M. D.; Harder, J.; Schroeder, D.; Brakhage, P. Loss of Phosphorus by Runoff For Agricultural Watersheds. *Soil Sci.* **2005**, *170* (7), 543–558.

(6) Sims, J. T.; Simard, R. R.; Joern, B. C. Phosphorus Loss in Agricultural Drainage: Historical Perspective and Current Research. *J. Environ. Qual.* **2010**. 27(2), 277.

(7) Ryther, J. H.; Dunstan, W. M. Nitrogen, Phosphorus, and Eutrophication in the Coastal Marine Environment 1008-1013. *Science* . **1971**. 171(3975), 1008–1013.

(8) Sharpley, A. N.; Chapra, S. C.; Wedepohl, R.; Sims, J.; Daniel, T. C.; Reddy, K. R.

Managing Agricultural Phosphorous for Protection of Surface Waters: Issues and Options. *J. Environ. Qual.* **1994**. 23(3), 437

(9) Conley, D. J.; Paerl, H. W.; Howarth, R. W.; Boesch, D. F.; Seitzinger, S. P.; Havens, K. E.; Lancelot, C.; Likens, G. E. Ecology - Controlling Eutrophication: Nitrogen and Phosphorus. *Science*. 2009.

(10) Correll, D. L. The Role of Phosphorus in the Eutrophication of Receiving Waters: A Review. *J. Environ. Qual.* **2010**.

(11) Elrashidi, M. A.; Mays, M. D.; Fares, A.; Seybold, C. A.; Harder, J. L.; Peaslee, S. D.; VanNeste, P. Loss of Nitrate-Nitrogen by Runoff and Leaching for Agricultural Watersheds. *Soil Sci.* **2005**.

(12) Elrashidi, M. A.; Mays, M. D.; Peaslee, S. D.; Hooper, D. G. A Technique to Estimate Nitrate-Nitrogen Loss by Runoff and Leaching for Agricultural Land, Lancaster County, Nebraska. *Commun. Soil Sci. Plant Anal.* **2004**.

(13) Minch, M. J. An Introduction to Hydrogen Bonding (Jeffrey, George A.). *J. Chem. Educ.* **2009**.

(14) Lam, H.-M.; Coschigano, K. T.; Oliveira, I. C.; Melo-Oliveira, R.; Coruzzi, G. M. Molecular-Genetics of Nitrogen Assimilation Into Amino Acids in Higher Plants. *Annu. Rev. Plant Physiol. Plant Mol. Biol.* **1996**.

(15) Cremer, P. S.; Flood, A. H.; Gibb, B. C.; Mobley, D. L. Collaborative Routes to Clarifying the Murky Waters of Aqueous Supramolecular Chemistry. *Nature Chemistry*. 2017.

(16) Hargrove, A. E.; Nieto, S.; Zhang, T.; Sessler, J. L.; Anslyn, E. V. Artificial Receptors for the Recognition of Phosphorylated Molecules. *Chemical Reviews*. 2011.

(17) Wang, Z.; Luecke, H.; Yao, N.; Quiocho, F. A. A Low Energy Short Hydrogen Bond in Very High Resolution Structures of Protein Receptor-Phosphate Complexes. *Nat. Struct. Biol.* **1997**.

(18) Neal, J. F.; Zhao, W.; Grooms, A. J.; Flood, A. H.; Allen, H. C. Arginine-Phosphate Recognition Enhanced in Phospholipid Monolayers at Aqueous Interfaces. *J. Phys. Chem. C* **2018**.

(19) Marcus, Y. Thermodynamics of Solvation of Ions. Part 5. - Gibbs Free Energy of Hydration at 298.15 K. *J. Chem. Soc. Faraday Trans.* **1991**.

(20) Kubik, S. Anion Recognition in Water. *Chemical Society Reviews*. 2010.

(21) Fumagalli, L.; Esfandiar, A.; Fabregas, R.; Hu, S.; Ares, P.; Janardanan, A.; Yang, Q.; Radha, B.; Taniguchi, T.; Watanabe, K.; et al. Anomalously Low Dielectric Constant of Confined Water. *Science (80-.).* **2018**.

(22) Ariga, K.; Tamagawa, H.; Inoue, Y.; Kunitake, T.; Sakurai, M. Theoretical Study of Intermolecular Interaction at the Lipid−Water Interface. 2. Analysis Based on the Poisson−Boltzmann Equation. *J. Phys. Chem. B* **2002**.

(23) Rumble, J. R. ed. Handbook of Chemistry and Physics 99th Edition.

(24) Sasaki, D. Y.; Kurihara, K.; Kunitake, T. Specific, Multiple-Point Binding of ATP and AMP to a Guanidinium-Functionalized Monolayer. *Journal of the American Chemical Society*. 1991.

(25) Dietrich, B.; Hosseini, M. W.; Lehn, J. M.; Sessions, R. B. Anion Receptor Molecules. Synthesis and Anion-Binding Properties of Polyammonium Macrocycles. *J. Am. Chem. Soc.* **1981**.

(26) Ariga, K.; Anslyn, E. V. Manipulating the Stoichiometry and Strength of Phosphodiester

Binding to a Bisguanidine Cleft in DMSO/Water Solutions. *J. Org. Chem.* **1992**.

(27) Kneeland, D. M.; Ariga, K.; Lynch, V. M.; Huang, C. Y.; Anslyn, E. V. Bis(Alkylguanidinium) Receptors for Phosphodiesters: Effect of Counterions, Solvent Mixtures, and Cavity Flexibility on Complexation. *J. Am. Chem. Soc.* **1993**.

(28) Dixon, R. P.; Geib, S. J.; Hamilton, A. D. Molecular Recognition: Bis-Acylguanidiniums Provide a Simple Family of Receptors for Phosphodiesters. *J. Am. Chem. Soc.* **1992**.

(29) Kalinin, S. V. Feel the Dielectric Force. *Science (80-.).* **2018**.

(30) Liu, Y.; Sengupta, A.; Raghavachari, K.; Flood, A. H. Anion Binding in Solution: Beyond the Electrostatic Regime. *Chem* **2017**.

(31) Israelachvili, J. N.; Pashley, R. M. Molecular Layering of Water at Surfaces and Origin of Repulsive Hydration Forces. *Nature* **1983**.

(32) Toney, M. F.; Howard, J. N.; Richer, J.; Borges, G. L.; Gordon, J. G.; Melroy, O. R.; Wiesler, D. G.; Yee, D.; Sorensen, L. B. Voltage-Dependent Ordering of Water Molecules at an Electrode-Electrolyte Interface. *Nature* **1994**.

(33) Velasco-Velez, J. J.; Wu, C. H.; Pascal, T. A.; Wan, L. F.; Guo, J.; Prendergast, D.; Salmeron, M. The Structure of Interfacial Water on Gold Electrodes Studied by X-Ray Absorption Spectroscopy. *Science (80-.).* **2014**.

(34) Lee, I. C.; Frank, C. W.; Yamamoto, T.; Tseng, H. R.; Flood, A. H.; Stoddart, J. F.; Jeppesen, J. O. Langmuir and Langmuir-Blodgett Films of Amphiphilic Bistable Rotaxanes. *Langmuir* **2004**.

(35) Jang, S. S.; Jang, Y. H.; Kim, Y. H.; Goddard, W. A.; Choi, J. W.; Heath, J. R.; Laursen, B. W.; Flood, A. H.; Stoddart, J. F.; Nørgaard, K.; et al. Molecular Dynamics Simulation of Amphiphilic Bistable [2]Rotaxane Langmuir Monolayers at the Air/Water Interface. *J.*

Am. Chem. Soc. **2005**.

(36) Cram, D. J. The Design of Molecular Hosts, Guests, and Their Complexes (Nobel Lecture). *Angewandte Chemie International Edition in English*. 1988.

(37) Schmidtchen, F. P.; Berger, M. Artificial Organic Host Molecules for Anions. *Chem. Rev.* **1997**.

(38) Onda, M.; Yoshihara, K.; Koyano, H.; Ariga, K.; Kunitake, T. Molecular Recognition of Nucleotides by the Guanidinium Unit at the Surface of Aqueous Micelles and Bilayers. A Comparison of Microscopic and Macroscopic Interfaces. *J. Am. Chem. Soc.* **1996**.

(39) Tohda, K.; Amemiya, S.; Ohki, T.; Nagahora, S.; Tanaka, S.; Bühlmann, P.; Umezawa, Y. Channel Mimetic Sensing Membranes for Nucleotides Based on Multitopic Hydrogen Bonding. *Isr. J. Chem.* **1997**.

(40) Beer, P. D.; Davis, J. J.; Drillsma-Milgrom, D. A.; Szemes, F. Anion Recognition and Redox Sensing Amplification by Self-Assembled Monolayers of 1,1'-Bis(Alkyl-N-Amido)Ferrocene. *Chem. Commun.* **2002**.

(41) Turygin, D. S.; Subat, M.; Raitman, O. A.; Selector, S. L.; Arslanov, V. V.; König, B.; Kalinina, M. A. Two-Dimensional Arrays of Amphiphilic Zn2+-Cyclens for Guided Molecular Recognition at Interfaces. *Langmuir* **2007**.

(42) Sovago, M.; Wurpel, G. W. H.; Smits, M.; Müller, M.; Bonn, M. Calcium-Induced Phospholipid Ordering Depends on Surface Pressure. *J. Am. Chem. Soc.* **2007**.

(43) Badis, M.; Tomaszkiewicz, I.; Joly, J. P.; Rogalska, E. Enantiomeric Recognition of Amino Acids by Amphiphilic Crown Ethers in Langmuir Monolayers. *Langmuir* **2004**.

(44) Blankenburg, R.; Meller, P.; Ringsdorf, H.; Salesse, C. Interaction between Biotin Lipids and Streptavidin in Monolayers: Formation of Oriented Two-Dimensional Protein

Domains Induced by Surface Recognition. *Biochemistry* **1989**.

(45) Mendelsohn, R. External Infrared Reflection Absorption Spectrometry of Monolayer Films at the Air-Water Interface. *Annu. Rev. Phys. Chem.* **2002**.

(46) Thomas, L. C.; Chittenden, R. A. Characteristic Infrared Absorption Frequencies of Organophosphorus Compounds—I The Phosphoryl (P□O) Group. *Spectrochim. Acta* **2002**.

(47) Thomas, L. C.; Chittekden, R. A. Characteristic Infrared Absorption Frequencies of Organophosphorus Compounds-VII. Phosphorns Ions. *Spectrochim. Acta Part A Mol. Spectrosc.* **1970**.

(48) Rudolph, W. W. Raman- and Infrared-Spectroscopic Investigations of Dilute Aqueous Phosphoric Acid Solutions. *Dalt. Trans.* **2010**.

(49) Ma, G.; Allen, H. C. DPPC Langmuir Monolayer at the Air-Water Interface: Probing the Tail and Head Groups by Vibrational Sum Frequency Generation Spectroscopy. *Langmuir* **2006**.

(50) Xiao, K. P.; Buhlmann, P.; Umezawa, Y. Ion-Channel-Mimetic Sensing of Hydrophilic Anions Based on Monolayers of a Hydrogen Bond-Forming Receptor. *Anal. Chem.* **1999**.

(51) Masayuki, D. Y.; Yanagi, M.; Kurihara, K.; Kunitake, T. The Interaction of a Guanidinium Monolayer with ATP and AMP, as Revealed by Surface Potential and UV Absorption Measurements. *Thin Solid Films* **1992**.

(52) Blondeau, P.; Segura, M.; Pérez-Fernández, R.; De Mendoza, J. Molecular Recognition of Oxoanions Based on Guanidinium Receptors. *Chem. Soc. Rev.* **2007**.

(53) Schug, K. A.; Lindner, W. Noncovalent Binding between Guanidinium and Anionic Groups: Focus on Biological- and Synthetic-Based Arginine/Guanidinium Interactions

with Phosph[on]Ate and Sulf[on]Ate Residues. *Chem. Rev.* **2005**.

(54) Tobey, S. L.; Anslyn, E. V. Energetics of Phosphate Binding to Ammonium and Guanidinium Containing Metallo-Receptors in Water. *J. Am. Chem. Soc.* **2003**.

(55) Linton, B.; Hamilton, A. D. Calorimetric Investigation of Guanidinium-Carboxylate Interactions. *Tetrahedron* **1999**.

(56) Berger, M.; Schmidtchen, F. P. The Binding of Sulfate Anions by Guanidinium Receptors Is Entropy-Driven. *Angew. Chemie - Int. Ed.* **1998**.

(57) Elsiddig, R.; Hughes, H.; Owens, E.; O'Reilly, N. J.; O'Grady, D.; McLoughlin, P. Kinetic and Thermodynamic Evaluation of Phosphate Ions Binding onto Sevelamer Hydrochloride. *Int. J. Pharm.* **2014**.

(58) Engel, T.; Reid, P. *Thermodynamics, Statistical Thermodynamics, & Kinetics*, Second Edi.; Kaveney, D., DuPont, C., Eds.; Pearson Education, 2010.

(59) Sharma, G.; First, E. A. Thermodynamic Analysis Reveals a Temperature-Dependent Change in the Catalytic Mechanism of Bacillus Stearothermophilus Tyrosyl-TRNA Synthetase. *J. Biol. Chem.* **2009**.

(60) Casillas-Ituarte, N. N.; Chen, X.; Castada, H.; Allen, H. C. Na+ and Ca2+ Effect on the Hydration and Orientation of the Phosphate Group of DPPC at Air - Water and Air - Hydrated Silica Interfaces. *J. Phys. Chem. B* **2010**.

(61) Chapman, A. C.; Thirlwell, L. E. Spectra of Phosphorus Compounds—I the Infra-Red Spectra of Orthophosphates. *Spectrochim. Acta* **2002**.

(62) Klähn, M.; Mathias, G.; Kötting, C.; Nonella, M.; Schlitter, J.; Gerwert, K.; Tavan, P. IR Spectra of Phosphate Ions in Aqueous Solution: Predictions of a DFT/MM Approach Compared with Observations. *J. Phys. Chem. A* **2004**.